Macroporous photonic crystal-based anti-ultraviolet and anti-near-infrared materials by doctor blade coating ⊘

Chang-Yun Cai; Kun-Yi Andrew Lin; Ying-Chu Chen; ... et. al

Check for updates

CrossMark

View Online

Export Citation

Articles You May Be Interested In

Macroporous photonic crystal-based anti-ultraviolet and anti-near-infrared materials by doctor blade coating

Chang-Yun Cai,[1] Kun-Yi Andrew Lin,[2] Ying-Chu Chen,[1] and Hongta Yang[1,a)]

[1]*Department of Chemical Engineering, National Chung Hsing University, 250 Kuo-Kuang Road, Taichung 40227, Taiwan*

[2]*Department of Environmental Engineering, National Chung Hsing University, 250 Kuo-Kuang Road, Taichung 40227, Taiwan*

In this article, we report a roll-to-roll compatible bottom-up self-assembly approach to fabricate double-multilayer macroporous polymer photonic crystals consisting of a multilayer of three-dimensional (3D) hexagonal close-packed (HCP) 200 nm spherical pores and a multilayer of 3D HCP 500 nm spherical pores. Both optical measurements and theoretical predictions reveal that the as-prepared polymer film exhibits anti-ultraviolet and anti-near-infrared properties caused by the Bragg's diffractive of incident ultraviolet radiation and near-infrared radiation from the crystalline lattice of air cavities in the polymer film. © *2016 AIP Publishing LLC.*
[http://dx.doi.org/10.1063/1.4941729]

The changes in the atmospheric composition and depletion of the stratospheric ozone during the past decades lead to an increase in solar ultraviolet (UV) and near-infrared (NIR) radiation dosage.[1–3] Prolonged human exposure to solar UV radiation causes deleterious health effects on the skin, eye and immune system.[4,5] The solar NIR rays generate radiant heat and are trapped inside buildings, resulting in a drastic increase of cooling loads.[6–8] However, most commercial polymers and glasses have poor UV and NIR reflectance quality.[9,10]

With a considerable interest, many studies have been recently reported on the preparation of UV-shielding or NIR-shielding materials via the structural design of polymer molecules, or addition of inorganic nanoparticles to polymeric matrix.[10–14] Unfortunately, the structural design of polymer molecules may cause changes in mechanical properties, causing huge inconvenience in polymer manufacturing.[10,11] Composites consisting of inorganic fillers provide attractive properties like resistance against UV radiation and NIR radiation.[12–14] However, it is still a challenge to achieve a homogeneous dispersion of the incorporated fillers in most polymeric matrices. The aggregation of inorganic nanoparticles with different refractive indices relative to the polymer results in light scattering, leading to translucent composite materials.

Photonic crystals are composed of periodic dielectric structures that provide a powerful platform for developing optical filters for prohibiting the propagation of a select frequency range of light.[15] Compared to the complex photolithography process, photonic crystals can be simply fabricated by colloidal self-assembly technologies.[16,17] Nonetheless, most self-assembly technologies have optical properties dominated by defects and cannot be favorable for industrial-scale mass fabrication.[18,19]

To resolve the scale-up issue of current bottom-up self-assembly technologies, a roll-to-roll compatible doctor blade coating technology has recently been developed to fabricate three-dimensional colloidal crystal-polymer composites in a single step.[20] This methodology is based on unidirectional shear aligning concentrated colloidal suspension, inspired by a spin-coating self-assembly technology.[21,22] After selectively removing colloidal crystals in the composite, the templating macroporous polymer films exhibit uniform diffractive colors. Here, we demonstrate that dual-doctor blade coated double-multilayer macroporous photonic crystals with a combination of anti-ultraviolet and anti-near-infrared properties can be fabricated.

The schematic illustration of the dual-doctor blade coating procedure for fabricating double-multilayer macroporous photonic crystals is displayed in Fig. 1. A 500 nm silica colloidal crystal-ETPTA (ethoxylated trimethylolpropane triacrylate) polymeric composite is doctor blade coated on an ETPTA wetting layer coated glass substrate (see supplementary material[23]). In a typical coating process, the 500 nm silica particles are dispersed in an ETPTA monomer to prepare for colloidal suspension with a particle volume fraction of 75%. An immobilized razor blade applies a uniform shear force to align silica microspheres when the substrate is moved at 1 mm/min. The monomer is photo-polymerized to
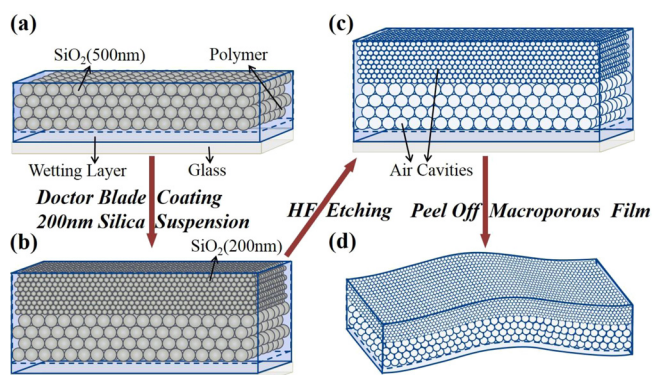

FIG. 1. The experimental procedure for fabrication of double-multilayer macroporous polymer photonic crystals.

a)Author to whom correspondence should be addressed. Electronic mail: hyang@dragon.nchu.edu.tw
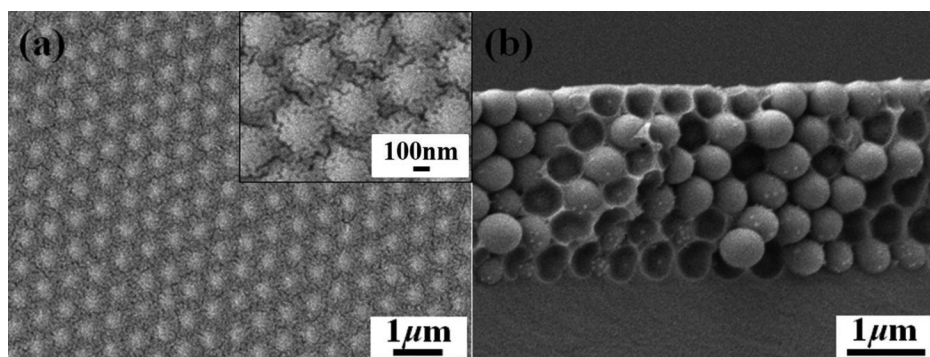
FIG. 2. A 500 nm silica colloidal crystal-polymer composite fabricated by the doctor blade coating technology. (a) Top-view SEM image. Inset shows a magnified SEM image. (b) Cross-sectional SEM image of the same sample as in (a).

form a 500 nm silica colloidal crystal-ETPTA polymeric composite. The substrate is subsequently doctor blade coated with a 200 nm silica colloidal crystal-ETPTA polymeric composite. The templating silica particles can be removed by etching in a 1 vol. % hydrofluoric acid aqueous solution. The resulting double-multilayer polymer film consisting of three-dimensional crystalline arrays of 500 nm air cavities and 200 nm air cavities can then be peeled off from the glass substrate to create self-standing macroporous polymer photonic crystals.

The hexagonal ordering of silica microspheres in the doctor blade coated 500 nm silica colloidal crystal-ETPTA polymeric composite is observed from the top-view SEM image (Fig. 2(a)). The protrusion depth of the top-layer silica microspheres from polymer matrix is smaller than the radius of silica microspheres, resulting in the non-close-packed appearance of silica microspheres. Indeed, the cross-sectional SEM image of the composite reveals the shear-aligned silica microspheres are three-dimensional close-packed and embedded in an ETPTA polymer matrix (Fig. 2(b)). This confirms that doctor blade coating technology can be utilized to create silica colloidal crystal-polymer composites.

The as-prepared 500 nm silica colloidal crystal-ETPTA polymer composite is subsequently doctor blade coated with a

200 nm silica colloidal crystal-ETPTA polymer composite. Fig. 3(a) displays a photograph of the as-prepared double-multilayer composite on a glass substrate illumined with white light. The composite exhibits a uniform blue color caused by the Bragg diffraction of incident visible light from the 200 nm silica crystalline lattice in the ETPTA polymer matrix. This indicates that the centimeter-sized 200 nm silica colloidal crystal-ETPTA composite can be doctor blade coated on polymeric composite substrate. The surface morphology of the double-multilayer composite as shown in Fig. 3(b) reveals that 200 nm silica microspheres are packed in a hexagonal ordering over tens of micrometers. Besides, both 200 nm and 500 nm silica microspheres are arranged into three-dimensional hexagonal ordered closed-packed colloidal crystals (Fig. 3(c)). Moreover, the bottom-multilayer composite does not collapse during the second doctor blade coating process. The magnified SEM image as shown in Fig. 3(d) also displays that the ordering of 200 nm microspheres on the contoured surface of 500 nm microspheres is evident and no considerable defects are observed on the interface. The result further discloses that multilayer colloidal crystal-polymer composites can be fabricated by a multiple-doctor blade coating process.

The templating silica particles in the double-multilayer composite can be completely etched. Compared with Fig. 3(a),
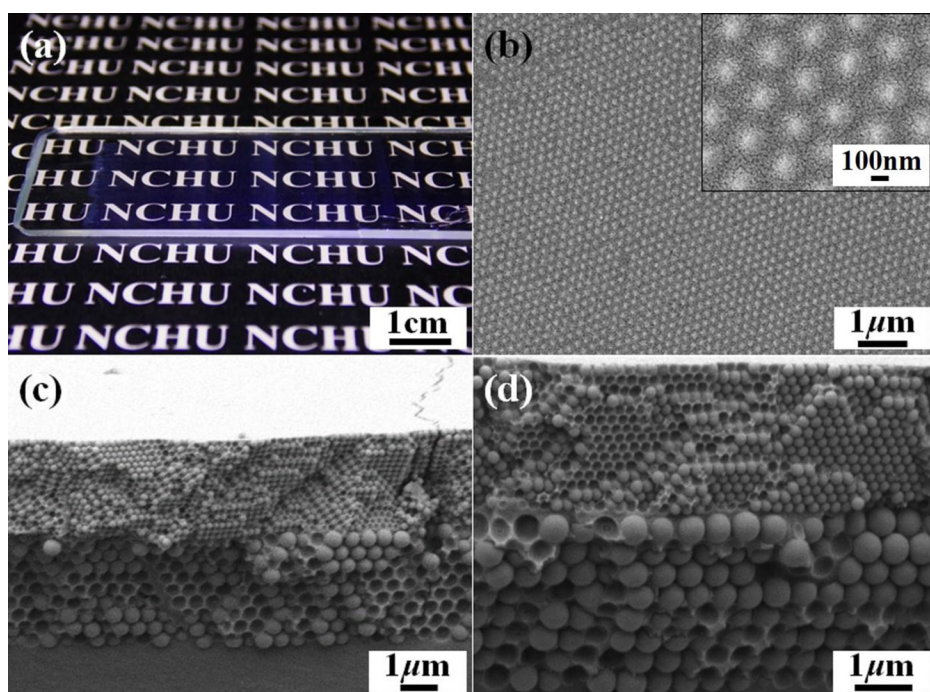

FIG. 3. A double-multilayer 200 nm and 500 nm silica colloidal crystal-polymer composite fabricated by the doctor blade coating technology. (a) Photograph of a glass slide (75 mm × 25 mm) coated with the double-multilayer composite. (b) Top-view SEM image of the sample in (a). (c) Cross-sectional SEM image of the sample in (a). (d) Magnified SEM image of (c).
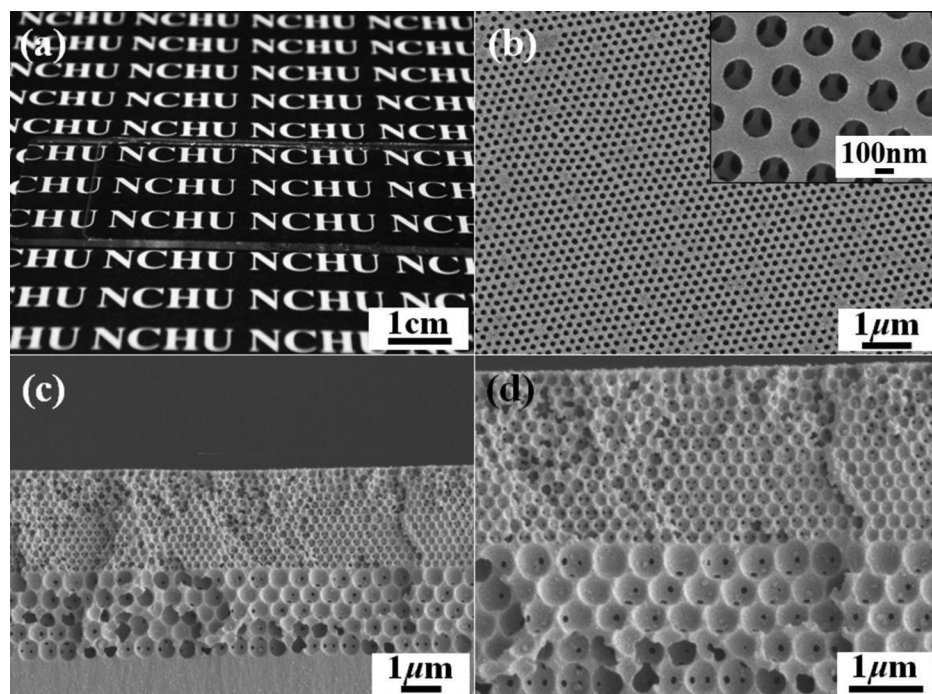
FIG. 4. A double-multilayer macroporous polymer film after the selective removal of templating 200 nm and 500 nm silica colloidal crystals. (a) Photographs of a glass slide (75 mm × 25 mm) coated with a double-multilayer ETPTA macroporous film. (b) Top-view SEM image of the sample in (a). (c) Cross-sectional SEM image of the sample in (a). (d) Magnified SEM image of (c).

the resulting macroporous polymer film templated from 200 nm and 500 nm silica colloidal crystals is colorless (Fig. 4(a)). The transparent sample indicates that incident visible light is not diffracted from the crystalline lattice of 200 nm and 500 nm air cavities in the polymer matrix. In Fig. 4(b), each 200 nm air void with an opening can be observed to be surrounded by six others in the top-view SEM image of the double-multilayer macroporous film, indicating that the surface is composed of a long-range hexagonal ordered air voids. Besides, the air voids are interconnected through small windows (insert of Fig. 4(b)) that originate from the touching sites of close-packed silica microspheres in the composite. The corresponding contact area between silica microspheres cannot be filled with the polymer matrix. A cross-sectional SEM image of the macroporous film as shown in Fig. 4(c) displays the three-dimensional orderings of 200 nm and 500 nm spherical air voids revealing that the double-multilayer macroporous structures do not collapse during the HF-etching procedure. It is also observed that both 200 nm air cavities and 500 nm air cavities in the ETPTA matrix are interconnected (Fig. 4(d)). This further demonstrates that the highly ordered 200 nm and 500 nm air cavities are face-centered cubic close-packed in the fabricated macroporous photonic crystals.

The resulting double-multilayer macroporous polymer films with a 1 mm thick wetting layer are then peeled off the glass substrate to create free-standing macroporous polymer photonic crystals. The film is optically clear and macroscopically uniform, (see supplementary material[23]). This indicates that large domain size transparent macroporous polymer films with three-dimensional crystalline arrays of pores can be fabricated by this coating technology.

To evaluate the optical properties of the doctor blade coated samples, the specular optical reflection and transmission are measured using UV-visible-near-IR spectrometers at normal incidence. As shown in Fig. 5(a), the featureless film exhibits around 5% reflectivity over the whole spectrum,

consistent with previous study.[24] The red dashed line shows the measured reflection peaks of the polymer composite located at 459 nm and 1153 nm. The low reflection amplitudes of the peaks result from the low refractive index contrast
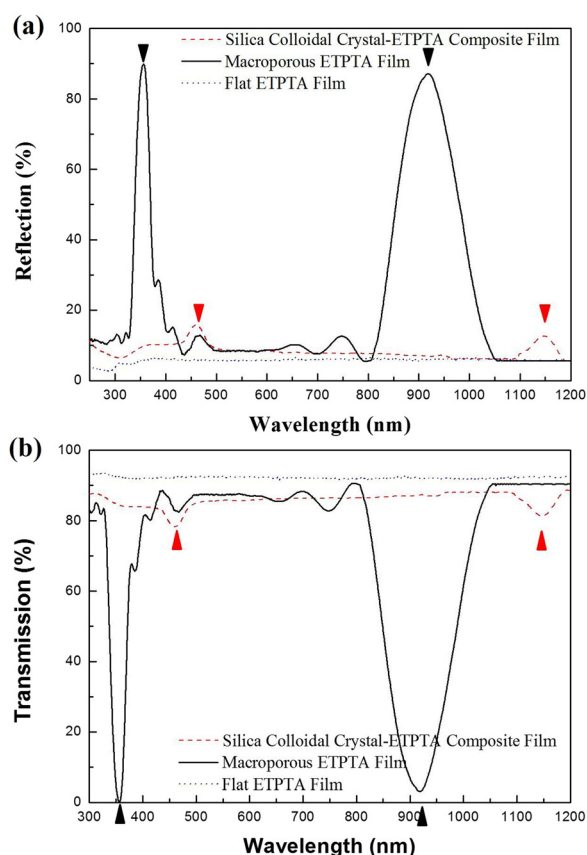

FIG. 5. (a) Optical reflection spectra, and (b) optical transmission spectra obtained from a flat ETPTA film, a silica-ETPTA composite consisting of 200 nm and 500 nm silica colloidal crystals, and a corresponding macroporous ETPTA film. The arrows indicate the expected positions of the peaks for each sample, calculated using Bragg's law.

between silica ($n_{silica} = 1.42$) and ETPTA ($n_{ETPTA} = 1.46$). In addition, the black solid line displays the measured reflection peaks of the corresponding macroporous ETPTA film located at 359 nm and 918 nm. The high refractive index contrast between air ($n_{air} = 1$) and ETPTA leads to over 90% reflection of incident ultraviolet radiation and over 85% reflection of incident near-IR radiation. Importantly, the reflection in visible light region is less than 10% in average, conforming that the macroporous film is highly transparent.

The positions of the four experimental reflection peaks are complemented by theoretical calculation using Bragg's law[25]

$$\lambda_{peak} = 2 n_{eff} d \, \sin \theta,$$

where n_{eff} is the effective refractive index of the medium, d is the interlayer spacing, and $\sin \theta = 1$ at normal incidence. The calculated reflection peak positions of the composite consisting of 200 nm silica colloidal crystals, the composite consisting of 500 nm silica colloidal crystals, the macroporous film templated from 200 nm silica microspheres, and the macroporous film templated from 500 nm silica microspheres locate at 463 nm, 1158 nm, 361 nm, and 903 nm, respectively. It is apparent that the theoretical reflection peak positions as shown by the indicating arrows are very close to the measured spectrum. This demonstrates that the doctor blade coated silica colloidal crystals and the corresponding macroporous polymer photonic crystals possess highly crystalline qualities. Besides, it is noted that the optical reflection spectrum of the double-multilayer macroporous film has features which correspond to peaks in each of the spectrum of the macroporous film with only one size of void (see supplementary material for more details[23]). This further suggests that the optical properties of the multilayer macroporous film can be approximated from the spectra of the individual layers by a simple superposition.

The transmission spectra of the samples are shown in Fig. 5(b). The double-multilayer composite film displays around 10% lower transmission in average over the whole spectrum as compared to the flat polymer film. That can be attributed to the presence of embedded silica colloidal crystals, since these can act as a strong scattering center, and therefore, cause lower optical transmittance.[26] Compared with that, the corresponding microporous film exhibits high transmission (over 85%) for a board band of visible wavelength as well as that of the flat polymer substrate, with less than 3% transmission in the ultraviolet radiation region and less than 5% transmission in the near-infrared radiation region. This suggests that doctor blade coated double-multilayer macroporous polymer photonic crystals can cause Bragg diffraction of incident ultraviolet radiation and near-infrared radiation from the close-packed 200 nm air cavities and 500 nm air cavities, respectively.

In summary, we have presented a scalable and roll-to-roll compatible colloidal self-assembly technology for fabricating double-multilayer macroporous photonic crystals. The macroporous films templated from three-dimensional 200 nm and 500 nm silica colloidal crystals are macroscopically transparent and can be used directly as large-area anti-ultraviolet and anti-near-infrared materials. The technique is compatible with standard industrial manufacturing and is promising for a variety of protective coatings.

[1]J. F. Bornman, P. W. Barnes, S. A. Robinson, C. L. Ballaré, S. D. Flinte, and M. M. Caldwell, Photochem. Photobiol. Sci. **14**, 88 (2015).

[2]F. S. Rowland, Philos. Trans. R. Soc. B **361**, 769 (2006).

[3]R. W. Portmann, J. S. Daniel, and A. R. Ravishankara, Philos. Trans. R. Soc. B **367**, 1256 (2015).

[4]R. M. Lucas, M. Norval, R. E. Neale, A. R. Young, F. R. de Gruijl, Y. Takizawag, and J. C. van der Leuni, Photochem. Photobiol. Sci. **14**, 53 (2015).

[5]K. Biniek, K. Levi, and R. H. Dauskardt, Proc. Natl. Acad. Sci. U. S. A. **109**, 17111 (2012).

[6]G. M. Revel, M. Martarelli, M. Á. Bengochea, A. Gozalbo, M. J. Orts, A. Gaki, M. Gregou, M. Taxiarchou, A. Bianchin, and M. Emiliani, Cem. Concr. Compos. **36**, 128 (2013).

[7]Y. Tian, W. Liu, T. H. Niu, C. H. Dai, X. Li, C. Cui, X. Zhao, Y. E., and H. Lu, Photochem. Photobiol. **90**, 1433 (2014).

[8]F. Causone, S. P. Corgnati, M. Filippi, and B. W. Olesen, Energy Build. **42**, 305 (2010).

[9]Y. Mastai, Y. Diamant, S. T. Aruna, and A. Zaban, Langmuir **17**, 7118 (2001).

[10]K. Adachi, M. Miratsu, and T. Asahi, J. Mater. Res. **25**, 510 (2010).

[11]T. V. Duncan, J. Colloid Interface Sci. **363**, 1 (2011).

[12]C. E. Small, S. Chen, J. Subbiah, C. M. Amb, S. Tsang, T. Lai, J. R. Reynolds, and F. So, Nat. Photonics **6**, 115 (2012).

[13]K. Xiong, L. Hou, M. Wu, Y. Hou, W. Mo, Y. Yuan, S. Sun, W. Xu, and W. Wang, Sol. Energy Mater. Sol. Cells **132**, 252 (2015).

[14]E. Tang, G. Cheng, X. Pang, X. Ma, and F. Xing, Colloid Polym. Sci. **284**, 422 (2006).

[15]K. Debnath, K. Welna, M. Ferrera, K. Deasy, D. G. Lidzey, and L. O'Faolain, Opt. Lett. **38**, 154 (2013).

[16]E. Istrate and E. H. Sargent, Rev. Mod. Phys. **78**, 455 (2006).

[17]P. Lodahl, S. Mahmoodian, and S. Stobbe, Rev. Mod. Phys. **87**, 347 (2015).

[18]J. Lee, J. Seo, D. Kim, S. Shin, S. Lee, C. Mahata, H. Lee, B. Min, and T. Lee, ACS Appl. Mater. Interfaces **6**, 9053 (2014).

[19]P. Jiang, G. N. Ostojic, R. Narat, and D. L. Mittleman, Adv. Mater. **13**, 389 (2001).

[20]C.-Y. Cai, K.-Y. Lin, and H. Yang, Appl. Phys. Lett. **105**, 201913 (2014).

[21]N. C. Linn, C. H. Sun, P. Jiang, and B. Jiang, Appl. Phys. Lett. **91**, 101108 (2007).

[22]C. H. Sun, P. Jiang, and B. Jiang, Appl. Phys. Lett. **92**, 061112 (2008).

[23]See supplementary material at http://dx.doi.org/10.1063/1.4941729 for schematic illustration of the experimental setup, a photograph of a double-multilayer ETPTA macroporous film, and optical reflection spectra obtained from macroporous ETPTA films.

[24]H. Guo, F. Zhang, G. Wu, F. Sun, X. Pu, X. Mai, and G. Qi, Opt. Mater. **22**, 269 (2003).

[25]P. Jiang, J. F. Bertone, K. S. Hwang, and V. L. Colvin, Chem. Mater. **11**, 2132 (1999).

[26]W. Caseri, Macromol. Rapid Commun. **21**, 705 (2000).